Modal Gain Analysis of Transverse Bragg Resonance Waveguide Lasers With and Without Transverse Defects

Lin Zhu, *Student Member, IEEE*, Axel Scherer, and Amnon Yariv, *Life Fellow, IEEE*

Abstract—We use a transfer matrix method to analyze the modal gain of transverse Bragg resonance (TBR) structures. We show that these TBR structures can support two types of modes characterized by different modal angles: small mode angle (SMA) modes and TBR modes. We discuss the origin, modal properties and field distributions of both the TBR modes and SMA modes. Three different feedback mechanisms are proposed to select the desired TBR modes.

Index Terms—Bragg gratings, modal control, semiconductor lasers.

I. INTRODUCTION

TOTAL internal reflection (TIR) is the most common waveguiding mechanism for semiconductor lasers. In these structures, single-mode operation at a particular wavelength can be achieved by controlling the refractive index difference between the waveguide core and cladding. For a large-area ($> 20\ \mu$m modal width) single-mode operation, a very small index contrast ($\Delta n < 10^{-4}$) is needed. The weak index difference makes the laser sensitive to fluctuations in its operating conditions that alter its refractive index profile.

In order to overcome this problem, waveguiding structures that use Bragg reflection from a periodic structure rather than TIR to confine light in the direction transverse to the propagation direction have been proposed and used for large-area, edge-emitting lasers [1]–[8]. These structures do not require very small index contrast and can be designed to have a single transverse mode that is distributed throughout the entire width of the laser for efficient and stable operation even at relatively high powers.

One example of these structures is the angled-grating distributed feedback (α-DFB) semiconductor laser proposed by Lang *et al.*, in which a uniform transverse grating provides the waveguiding mechanism and the angle facet selects the desired modes [1], [2]. Another example proposed by Yariv uses a guiding channel sandwiched between two gratings [3]. The guiding channel is a "defect" in the grating and can suppress radiation loss. In these grating waveguide structures, a resonance condition needs to be satisfied in the transverse direction to support a low-loss optical mode. Here, we generalize these two examples as transverse Bragg resonance (TBR) structures, and we refer to the modes that depend on the transverse grating resonance as TBR modes.

However, in these structures, modes which are not guided by the transverse grating can also lase when gain is provided. First, effective index-guided modes can exist due to TIR when the cladding index is smaller than the low index region of the transverse grating. Second, low-loss leaky modes due to incomplete TIR (gain-guided modes) can exist in these wide waveguide structures regardless of the cladding index. Thus, we need a formalism that accounts for all the modes of the structure as well as their losses. For the practical laser design based on the transverse Bragg reflection, we also need to engineer the grating guided modes to be the preferred modes.

In this paper, we use a transfer matrix method (TMM) to analyze the modal gain of all the possible modes supported by the TBR waveguide with and without a "defect." We compare different low-loss optical modes for these two structures. We show that gain modulation in the transverse direction can also guide TBR modes. We conclude by suggesting three different feedback mechanisms that can be used to ensure the lasing of TBR modes only.

II. THEORETICAL APPROACHES

Fig. 1 shows the TBR structures without and with a defect. In Fig. 1(a), the TBR structure consists of uniform Bragg reflectors in the transverse direction. In Fig. 1(b), a defect core (with refractive index n_{co} and width W_d) is present at the center of the grating. The Bragg reflectors consist of alternating high and low index layers with refractive indexes n_h and n_l, respectively. The refractive index outside the waveguide region is n_{out}. The grating has N layers, a period b and a duty cycle d. We define the average index of the grating n_{avg} as: $n_{\mathrm{avg}} = n_h \cdot d + n_l \cdot (1 - d)$. The refractive index of the defect core n_{co} is designed to be n_h or n_l. In accordance with the round-trip resonance condition and the phase of reflection from the grating, for a mode to be supported by the defect, $W_d = (m + 1/2)b$, where m is an integer [3].

According to the coupled-mode analysis, light can be confined by the transverse Bragg grating when its transverse wavevector matches the grating vector. Therefore, we can define the transverse resonance angle for both structures as [3], assuming that the first order Bragg reflection is used

$$\theta_{\mathrm{res}} = \cos^{-1}\left[\frac{\sqrt{\left(\frac{2\pi n_{\mathrm{avg}}}{\lambda}\right)^2 - \left(\frac{\pi}{b}\right)^2}}{\left(\frac{2\pi n_{\mathrm{avg}}}{\lambda}\right)}\right]. \tag{1}$$
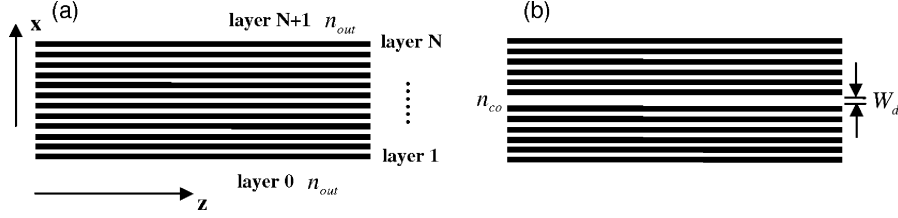
Fig. 1.   Transverse Bragg resonance structures (a) without a defect core (b) with a defect core.
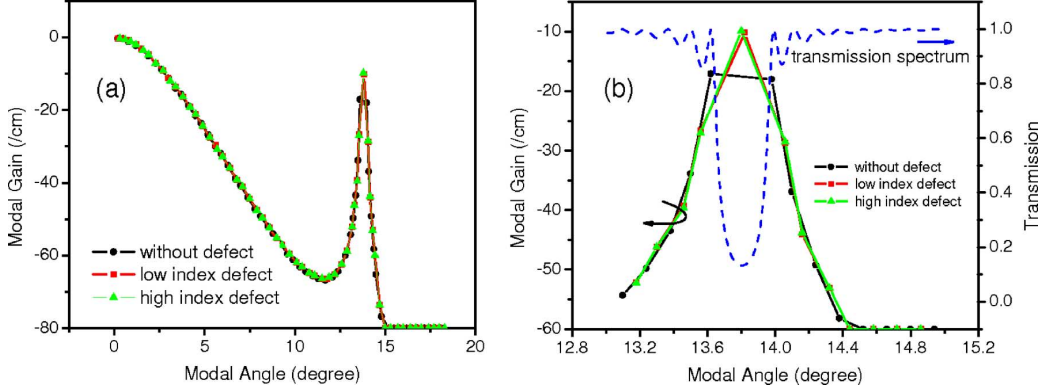

Fig. 2.   (a) Modal gain (loss) versus modal angle for passive TBR waveguides with and without a defect. (b) Modal gain of TBR modes near the resonance angle (solid lines) and the transmission spectrum of the grating (the dashed line).

The grating coupling constant around the resonance can be calculated as [9], [10]

$$\kappa_{\text{index}} = \left(\frac{2b}{\lambda^2}\right)(n_h^2 - n_l^2)\sin(\pi d). \quad (2)$$

Our analysis is based on the TMM proposed in [1]. In this approach, the structure is considered to consist of a series of dielectric layers, each characterized by a label $n = 0, 1, \ldots, N, N+1$ (see Fig. 1). We assume a wave propagating in the positive z direction has a spatial dependence $\exp(-i\beta z)$, where β is a real or complex constant. In each layer, the electrical field can be written as the sum of the forward-going ($E_{f,n,+x}$) and backward-going waves ($E_{b,n,-x}$)

$$E(x) = E_{f,n}\exp(-ik_n(x - x_n)) + E_{b,n}\exp(ik_n(x - x_n))$$
$$k_{s,n} = \frac{2\pi n_n}{\lambda} + ig_n \qquad k_n = \sqrt{k_{s,n}^2 - \beta^2} \quad (3)$$

where $k_{s,n}$ is the wavevector for the plane wave in each layer with gain g_n and x_n is the x coordinate of the start of the nth layer. We can relate the field and its derivative within a layer to the coefficients by a matrix

$$\begin{pmatrix} E_n(x) \\ E_n'(x) \end{pmatrix} = T_n(x - x_n) \cdot \begin{pmatrix} E_{f,n} \\ E_{b,n} \end{pmatrix}$$
$$T_n(x) = \begin{pmatrix} \exp(-ik_nx) & \exp(ik_nx) \\ -ik_n\exp(-ik_nx) & ik_n\exp(ik_nx) \end{pmatrix}. \quad (4)$$

Since β is the same for all the layers, we can match the field and its derivative at every interface and propagate the field from layer 0 to layer $N+1$. We self-consistently solve for the field distribution where the field outside the cladding layers is purely outgoing. The corresponding boundary condition for the TMM is $E_{f,0} = 0$ and $E_{b,N+1} = 0$. Satisfying this boundary condition gives a series of β.

A lossless optical mode corresponds to a real β. In our structures, lossless modes are the effective index-guided modes. A complex β corresponds to a leaky mode and this mode experiences an exponential decay of the field amplitude in the propagation direction and an exponential increase in the transverse direction of the cladding region. This means that a complex β is not a physical solution of Maxwell's equations since the field amplitude increases to infinity at the transverse direction. However, when gain is provided for the grating region to exactly compensate the waveguiding loss, β becomes real and the field amplitude remains constant in the propagation direction. Thus, in our approach, the imaginary part of β corresponds to the gain required to support a lossless optical mode with its propagation constant equal to the real part of β. So we define the real part of β as the phase propagation constant and the imaginary part as the modal gain (threshold gain) and consider the corresponding field distribution as the mode for the waveguide. Negative modal gain is equivalent to modal loss. We also define the modal angle as $\theta = \cos^{-1}(\text{Re}(\beta)/(2\pi n_{\text{avg}}/\lambda))$. Using this method, we can account for both lossless modes and leaky modes. In the following discussion, we show that losses for leaky modes can be very small and thus all these modes can lase when gain is provided.

III. TBR STRUCTURES WITH AND WITHOUT A DEFECT

First, to compare the performance of the TBR structures with and without a defect, we calculate the modal gain for each mode as a function of the modal angle for three different passive structures in Fig. 2. We assume: $n_h = 3.25$; $n_l = 3.245$; $d = 0.5$; $n_{\text{out}} = 3.25$; $b = 1\ \mu\text{m}$; $W_d = 0.5\ \mu\text{m}$; $N = 100$; $\lambda =$
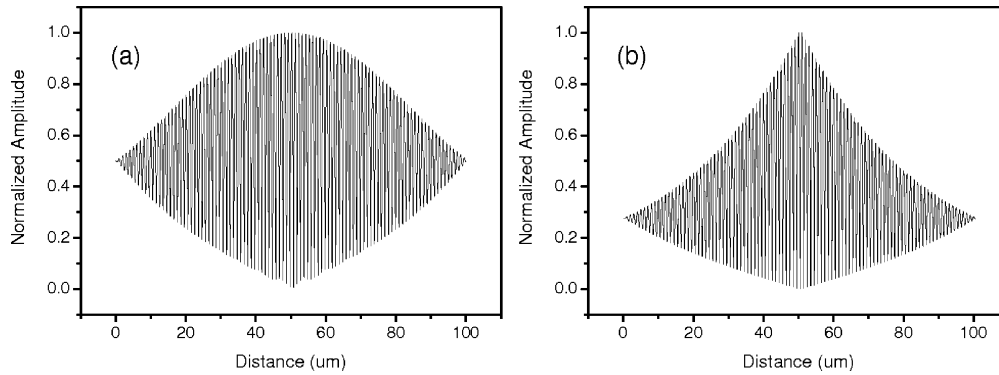
Fig. 3. Normalized field amplitude. (a) Lowest loss TBR mode (no defect) with 13.63° modal angle and 16.88/cm loss. (b) Lowest loss TBR mode (high-index defect) with 13.80° modal angle and 9.94/cm loss.
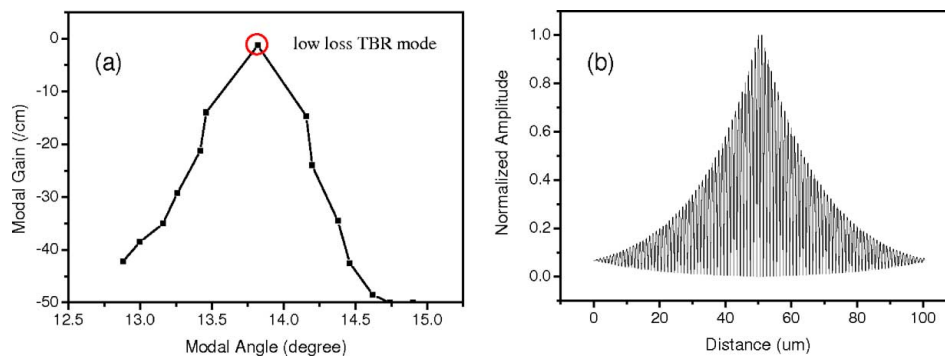

Fig. 4. (a) Modal gain (loss) versus modal angle for the TBR waveguide with a high-index defect. (b) Electric field amplitude of the corresponding lowest loss TBR mode. All the simulation parameters are the same as in Fig. 2 except $n_l = 3.24$.

1.55 μm. Therefore, the resonance angle calculated from (1) is 13.8° and the coupling constant calculated from (2) is 270/cm.

As shown in Fig. 2, in all the structures considered, the modes with small modal angles experience zero or very low radiation loss. We call these modes small modal angle (SMA) modes. SMA modes include both lossless effective index-guided modes and low loss leaky modes. They are almost parallel to the grating and do not radiate significantly. SMA modes will be discussed in details in Section V. As the modal angle increases, all the modes experience higher radiation loss. However, around the transverse resonance angle of 13.8°, low loss modes exist. These modes are supported by the transverse grating and are therefore the TBR modes. For a finite structure, TBR modes are leaky due to nonunity grating reflectivity. Compared to the SMA modes, TBR modes have much larger intermodal discrimination between the lowest loss and the next lowest loss modes, which is the key in realizing a single transverse mode operation.

Fig. 2(b) shows the modal gain for the modes near the TBR angle. We also plot the transmission spectrum of the grating at different modal angles to illustrate the relationship between the location of TBR modes and the stop band of the grating. For the TBR waveguide without a defect (the line with circles), the two lowest loss modes are located on either side of the stop band of the grating, similar to a longitudinal DFB structure. While for the TBR waveguide with a defect (the lines with squares and triangles), the lowest loss mode is in the middle of the stop band of the grating, similar to a longitudinal DFB structure with a π

phase slip [10]. The defect TBR modes experience about 7/cm less radiation loss compared to the lowest loss modes of the same TBR waveguide without a defect. The modal loss profiles are similar between the TBR waveguides with a low index defect and a high index defect. For these two structures, the modal angles of the lowest loss TBR modes are both 13.8°, which match the prediction from the coupled-mode analysis in (1).

In Fig. 2(b), the allowed modal angles of the TBR modes correspond to the discrete transmission peaks (without a defect) and dips (with a defect) of the grating transmission spectrum. TBR structures with and without defects support multiple Bragg-guided modes because the finite device width imposes a second transverse resonance condition and thus leads to the mode splitting. For all the three cases we discussed, the gain difference between the lowest loss TBR modes and the next lowest loss TBR modes is as high as 17/cm.

Fig. 3 shows the normalized electric field amplitudes for different lowest loss TBR modes. The modes possess a "fast" spatial oscillation due to the grating. Since the field in the cladding is assumed to be purely outgoing, the energy leaks out at two boundaries ($x = 0$ and $x = 100 \mu$m). In Fig. 3, it is clear that the more confined mode has relatively smaller amplitude at the boundary.

We can reduce the loss of TBR modes to be almost zero through the grating design. In Fig. 4, we show the modal gain and the field profile of the lowest loss TBR mode for such a design. The design is for the TBR waveguide with a high-index
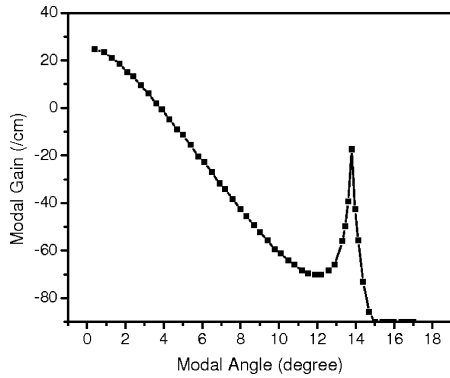
Fig. 5. Modal gain (loss) versus modal angle for a gain-guided TBR waveguide.
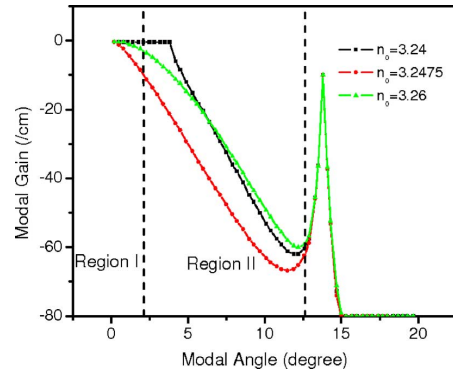

Fig. 6. Modal gain (loss) versus modal angle for the passive TBR waveguide with different outside claddings. All simulation parameters are the same as in Fig. 2 except n_{out}.
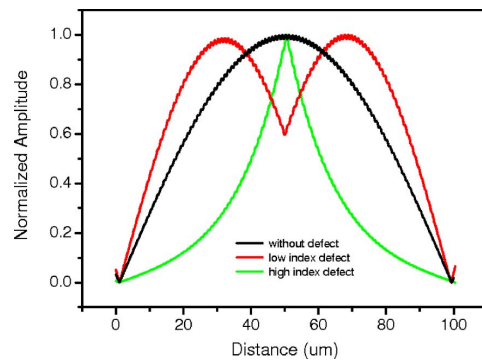
defect and all the parameters are the same as in Fig. 2 except $n_l = 3.24$. The coupling constant of this grating is 540/cm, much higher than the one in Fig. 2. Thus, we can obtain a more confined TBR mode. In Fig. 4, the radiation loss for the lowest loss TBR mode is about 1/cm.

IV. PERIODIC GAIN-GUIDED TBR WAVEGUIDES

Periodic gain (loss) modulation in the transverse direction can also support TBR modes. For the transverse gain-modulated grating structure, we assume that the refractive index is the same everywhere and the grating alternates between a high-gain layer with g_h and a low-gain layer with g_l. There is no defect in this gain grating. The grating, as in the above example, has N layers, a period b, and a duty cycle d. We calculate the modal gain of all the modes for this transverse gain-modulated structure in Fig. 5. The simulation parameters are as follows: $g_h = 50/\text{cm}$; $g_l = 0$; $n_{\text{background}} = 3.2475$; $d = 0.5$; $b = 1\ \mu\text{m}$; $N = 100$; and $\lambda = 1.55\ \mu\text{m}$.

We obtain both SMA modes and TBR modes for the gain-coupled TBR waveguide as well. The lowest loss mode of TBR modes is exactly located at the $13.8°$ transverse resonance angle predicted by the coupled-mode theory, similar to a pure gain-coupled DFB structure [9]. Since gain is provided for the waveguide, SMA modes possess positive modal gains. On the contrary, the lowest loss TBR mode still experience about 20/cm radiation loss. This means that the confinement for this gain coupled grating is not very strong. The coupling constant for the gained coupled grating can be calculated as: $\kappa_{\text{gain}} = (2b/\lambda)(g_h - g_l)\sin(\pi d)/\pi$ [9]. In the example above, the gain coupling constant is about 20.5/cm, which is much smaller than the coupling constant of the index-coupled grating in Fig. 2.

V. SMALL MODAL ANGLE (SMA) MODES

SMA modes possess zero or very small radiation losses and compete with the desired TBR modes when gain is provided. The layers outside the grating strongly interact with SMA modes since they propagate almost parallel to the grating. In Fig. 6, we show the modal gain of both the SMA and TBR modes for a high-index defect TBR waveguide with different values of n_{out}. The three lines correspond to the situation when the cladding index is smaller than, equal to, and larger than the

Fig. 7. Normalized electric field amplitudes of the lossless effective index guided modes when the outside cladding index $n_{out} = 3.24$. Other simulation parameters are the same as in Fig. 2.

average index of the grating, respectively. When the cladding index is the same as the average index of the grating, the SMA modes experience the highest radiation loss.

There are several origins for the SMA modes. First, lossless effective index-guided waveguide modes can exist when the cladding index is less than the low-index region of the grating (n_l). In this case $(n_{out} = 3.24$, Fig. 6), the propagation constant β is a real number and satisfies the condition $2\pi n_l/\lambda < \beta < 2\pi n_h/\lambda$. Thus, the field is guided in the high-index regions of the grating and is evanescent in the low-index regions of the grating and the cladding. In Fig. 7, we plot such fields for three different situations: no defect, high-index defect and low-index defect. The field distribution has a strong dependence on the defect. In contrast to the TBR modes shown in Figs. 3 and 4, the field profiles of the effective index-guided SMA modes only have very small amplitude oscillations corresponding to the grating period on top of the overall slowly varying envelope.

As the cladding index increases ($n_{out} = 3.2475$ and $n_{out} = 3.26$, Fig. 6), these modes become leaky and their propagation constants become complex numbers. If the condition $2\pi n_l/\lambda < \text{Re}(\beta) < 2\pi n_h/\lambda$ is satisfied (Region I in Fig. 6), the radiation loss for these modes is small. This is because that the Fresnel reflectivity at the interfaces approaches unity when the angle of incidence reaches $90°$ ($0°$ modal angle). Thus, the losses due to incomplete TIR from the dielectric interfaces are expected
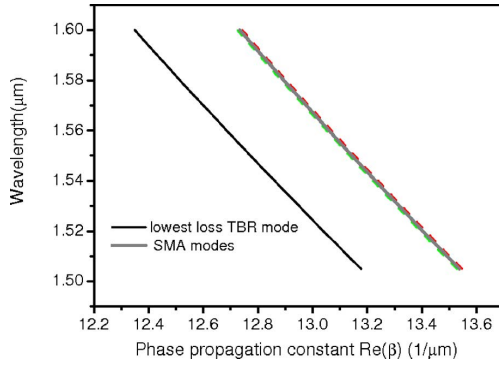
Fig. 8. Dispersion relation of the lowest loss TBR mode (the black line) and SMA modes (the gray region). There are six lines in the gray region, and each of them corresponds to one particular SMA mode. All simulation parameters are the same as in Fig. 4.

Fig. 9. (a) Angled facet with a tilt angle θ. (b) r_f for all the modes with different modal angles.

to be small when the light is at grazing incidence. In [11], it is also shown that the radiation loss for these modes becomes smaller as the total waveguide width increases. The field distributions of the lowest loss (order) leaky SMA modes are similar to the corresponding lossless effective index-guided modes in Fig. 7. When the modal angle is larger than this range (Region II, $\mathrm{Re}(\beta) < 2\pi n_l/\lambda$), the radiation loss becomes high unless the mode can be guided by the grating.

Now, it is clear that TBR structures support two kinds of modes: TBR modes and SMA modes. TBR modes are supported by the Bragg reflection of the transverse grating. The loss difference between the lowest loss (order) and the next lowest loss TBR modes is high. SMA modes include lossless effective index-guided modes and leaky modes with small modal angles. The existence of lossless effective index-guided waveguide modes depends on the cladding index, while leaky modes with small modal angles exist regardless of the cladding index. The loss difference among all the SMA modes is small. In Fig. 8, we plot the dispersion relation of the lowest loss TBR mode and six lowest loss (order) SMA modes for a passive TBR waveguide. The loss for the TBR mode is about 1/cm, and losses for the SMA modes are all less than 2/cm.

When gain is provided for a TBR waveguide, the lowest loss TBR modes and SMA modes have similar gains. Thus, the TBR modes and SMA modes compete with each other and both of them can lase.

VI. FEEDBACK MECHANISMS FOR TBR LASERS

Thus far, we have only discussed TBR waveguides. To analyze lasers, we must include the effect of the feedback mechanism that defines the resonator. To ensure a single transverse mode operation near the Bragg resonance, the feedback mechanism needs to be tailored. Compared to SMA modes, TBR modes have a much "faster" spatial oscillation in the transverse direction. Thus, if we can integrate a spatial filter at the facet to favor the fast spatial oscillation, TBR modes can be preferred. Angled facets were proposed in [1] to realize this goal. The angled facets act exactly like a spatial filter and the feedback from the facet will only be provided for the mode whose modal angle is very close to the tilt angle.
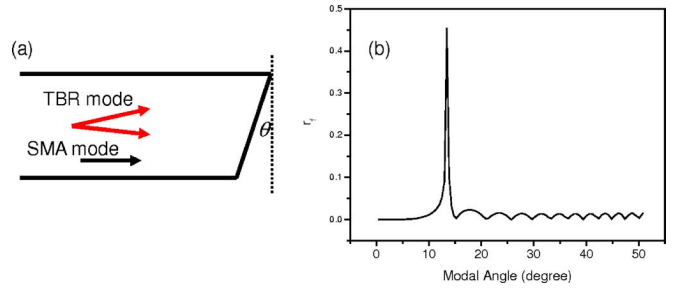
The reflectivity of different modes at an angled facet can be calculated using the model in [12]

$$R = R_f(\theta) \cdot A \cdot r_f \text{ with } r_f = \mathrm{Re}(\beta) \int_{-\infty}^{+\infty} |E|^2 \, e^{i2\theta \mathrm{Re}(\beta)x} dx$$

(5)

where x is the transverse coordinate, θ is the tilt angle for the facet (see. Fig. 9) and $R_f(\theta)$ is the Fresnel reflection coefficient of the dielectric interface between semiconductor and air. A is a constant. In Fig. 9, we calculate r_f in the (5) for all the normalized modes with different modal angles of the TBR waveguide described in Fig. 4. The tilt angle θ is assumed to be $13.8°$ in the calculation. r_f in the (5) possesses a maximum value for the mode with a modal angle same as the tilt angle θ. The reflectivity for the TBR modes thus can be designed to be maximum by choosing the tilt angle θ to be the same as the resonance angle θ_{res}. While for the SMA modes, in the (5) is almost zero. Therefore, these modes are not reflected by the facet. Indeed, the angled facet is a spatial filter which gives the strongest reflection for the mode with a modal angle same as the tilt angle.

A second approach is to coat the facet in a way such that the reflection for the modes with small modal angles is almost zero while the reflection for the modes around the transverse resonance angle is high. Thus, similar selection mechanism can be achieved as an angled facet design. Since the modal angle difference between the SMA modes and TBR modes are large, a typical single layer antireflection coating can achieve this goal, as shown in Fig. 10.

In Fig. 10(a), the laser facet is coated with a dielectric layer with a refractive index n_c and thickness h. Details of the antireflection coating design can be found in [13]. Here, we optimize our antireflection design for the mode with $0°$ modal angle. Thus, we have

$$n_c = \sqrt{n_{\mathrm{avg}} n_{\mathrm{air}}}, \quad h = \frac{\lambda}{4n_c}$$

(6)

where n_{air} is the refractive index of air and λ is the wavelength. Given $n_{\mathrm{air}} = 1$, $n_{\mathrm{avg}} = 3.245$, and $\lambda = 1.55 \ \mu\mathrm{m}$, we calculate the reflectivity for all the modes with different modal angles in Fig. 10(b). When the modal angle is less than $2°$, the reflectivity of all the calculated modes is smaller than $2*10-3$. Thus, the SMA modes can not obtain enough feedback from the facet. While for the TBR modes (modal angle $\sim 13.8°$), the reflectivity is around 0.18, two orders higher than the SMA modes.
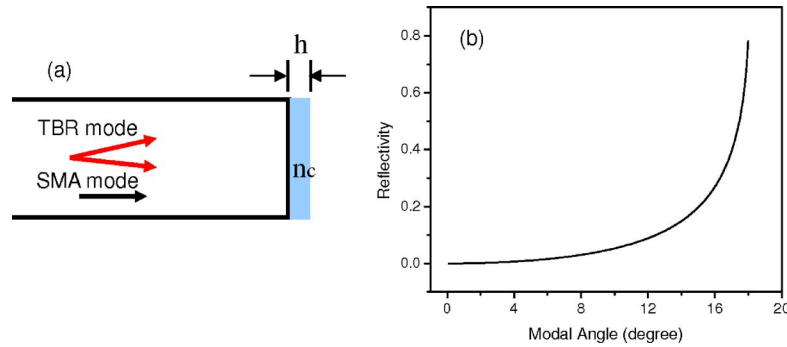
Fig. 10. (a) Coated facet design. The coating layer has a refractive index n_c and thickness h. (b) Reflectivity for all the modes with different modal angles.

Since the SMA modes and TBR modes are the only two kind low loss modes supported by the structure, the coating layer can effectively discriminate against the SMA modes and ensure the lasing in the TBR modes.

The third way is to introduce a second grating in the longitudinal direction to select the propagation constant corresponding to the TBR mode [4], [6], [14], [15]. We have demonstrated the lasing in the TBR modes based on this approach in [16]. In [16], we have systematically tuned the lasing wavelength by changing both the transverse and longitudinal lattice constants, which proves that the lasing mode is guided by the TBR and the feedback is provided by the longitudinal Bragg resonance. It should be pointed out that the angled facet design was also used to suppress the SMA modes and provide a singled-lobed far-field output. However, the facet reflection is not the feedback mechanism. Thus, the tilt angle does need to be the transverse resonance angle and the exact value is not critical, which is different from the first approach.

VII. CONCLUSION

In summary, we use a TMM to analyze the modal gain and field distribution for different modes supported by TBR structures with and without transverse defects. TBR modes are guided by the Bragg reflection of the transverse grating and the large modal discrimination of TBR modes is ideal for the design of single transverse mode large-area lasers. TBR waveguides without a defect support band-edge modes, while TBR waveguides with a defect support bandgap modes and the defect can suppress the radiation loss. SMA modes include effective index-guided modes and gain-guided leaky modes with small modal angles and they exist in most large-area waveguide structures. Three feedback mechanisms including angled facets, antireflection coating, and an additional longitudinal grating are proposed to select the preferred TBR modes.

ACKNOWLEDGMENT

REFERENCES

[1] R. J. Lang, K. DZurko, A. Hardy, S. Demars, A. Schoenfelder, and D. Welch, "Theory of grating-confined broad-area lasers," *IEEE J. Quantum Electron.*, vol. 34, no. 11, pp. 2196–2210, Nov. 1998.

[2] A. M. Sarangan, M. W. Wright, J. Marciante, and D. J. Bossert, "Spectral properties of angles-grating high-power semiconductor lasers," *IEEE J. Quantum Electron.*, vol. 35, no. 8, pp. 1220–1230, Aug. 1999.

[3] A. Yariv, "Coupled-wave formalism for optical waveguiding by transverse Bragg reflection," *Opt. Lett.*, vol. 27, pp. 936–938, 2002.

[4] C. S. Kim, W. W. Bewley, C. L. Canedy, I. Vurgaftman, M. Kim, and J. R. Meyer, "Broad-stripe near-diffraction-limited midinfrared laser with a second-order photonic-crystal distributed feedback grating," *IEEE Photon. Technol. Lett.*, vol. 16, no. 5, pp. 1250–1252, May 2004.

[5] J. M. Choi, L. Zhu, W. Green, G. DeRose, A. Yariv, "Large-area semiconductor transverse Bragg resonance (TBR) lasers for efficient, high power operation," presented at the 24th ICALEO 2005, #406.

[6] L. Zhu, J. M. Choi, G. A. DeRose, A. Yariv, and A. Scherer, "Electrically pumped two-dimensional Bragg grating lasers," *Opt. Lett.*, vol. 31, pp. 1863–1865, 2006.

[7] W. W. Bewley, I. Vurgaftman, R. E. Bartolo, M. J. Jurkovic, C. L. Felix, J. R. Meyer, H. Lee, R. U. Martinelli, G. W. Tuner, and M. Manfra, "Limitations to beam quality of midIR angled-grating distributed feedback lasers," *IEEE J. Sel. Topics Quantum Electron.*, vol. 7, no. 2, pp. 96–101, Mar./Apr. 2001.

[8] K. Paschke, A. Bogatov, F. Bugge, A. E. Drakin, J. Fricke, R. Guther, A. A. Stratonnikov, H. Wenzel, and G. Erbert, "Properties of ion-implanted high-power anged-grating distributed-feedback lasers," *IEEE J. Sel. Topics Quantum Electron.*, vol. 9, no. 5, pp. 1172–1178, Sep./Oct. 2003.

[9] H. Kogelnik and C. V. Shank, "Coupled-wave theory of distributed feedback lasers," *J. Appl. Phys.*, vol. 43, pp. 2327–2335, 1971.

[10] H. A. Haus and C. V. Shank, "Antisymmetric taper of distributed feedback lasers," *IEEE J. Quantum Electron.*, vol. QE-12, no. 9, pp. 532–539, Sep. 1976.

[11] A. Yariv and P. Yeh, *Optical Waves in Crystals*. Singapore: Wiley Interscience, 2003, ch. 11.11.

[12] D. Marcuse, "Reflection loss of laser mode from tilted end mirror," *J. Lightw. Technol.*, vol. 7, no. 2, pp. 336–339, Feb. 1989.

[13] G. R. Fowles, *Introduction to Modern Optics*. Boston, MA: Dover, 1989, ch. 4.4.

[14] K. M. Dzurko, A. Hardy, D. R. Scifres, D. F. Welch, R. Waarts, and R. Lang, "Distributed Bragg reflector ring oscillators: A large aperture source of high single-mode optical power," *IEEE J. Quantum Electron.*, vol. 29, no. 6, pp. 1895–1905, Jun. 1993.

[15] I. Vurgaftman and J. R. Meyer, "Photonic-crystal distributed-feedback quantum cascade lasers," *IEEE J. Quantum Electron.*, vol. 38, no. 6, pp. 592–602, Jun. 2002.

[16] L. Zhu, G. A. DeRose, A. Scherer, and A. Yariv, "Electrically pumped, edge-emitting photonic crystal lasers with angled facets," *Opt. Lett.*, vol. 32, pp. 1256–1258, 2007.

Lin Zhu (S'06) received the B.S. and M.S. degrees in electrical engineering from Tsinghua University, Beijing, China, in 2000 and 2002, respectively. He received the M.S. degree in electrical engineering from California Institute of Technology, Pasadena, in 2004, where he is currently working toward the Ph.D. degree in electrical engineering.

His research interests include semiconductor lasers, periodic photonic structures, and optical resonators.

Axel Scherer received the B.S., M.S., and Ph.D. degrees from the New Mexico Institute of Mining and Technology, Socorro, in 1981, 1982, and 1985, respectively.

From 1985 to 1993, he worked in the Quantum Device Fabrication Group at Bellcore. Currently, he is the Bernard E. Neches Professor of electrical engineering, applied physics, and physics at the California Institute of Technology, Pasadena, specializing in device microfabrication. His research interests include design and fabrication of functional photonic, nanomagnetic, and microfluidic devices.

Amnon Yariv (S'56–M'59–F'70–LF'95) received the B.S., M.S., and Ph.D. degrees in electrical engineering from the University of California, Berkeley, in 1954, 1956, and 1958, respectively.

In 1959, he joined Bell Telephone Laboratories, Murray Hill, NJ. In 1964, he joined the California Institute of Technology (Caltech), Pasadena, as an Associate Professor of electrical engineering, becoming a Professor in 1966. In 1980, he became the Thomas G. Myers Professor of electrical engineering and applied physics. In 1996, he became the Martin and Eileen Summerfield Professor of applied physics and Professor of electrical engineering. On the technical and scientific sides, he took part (with various co-workers) in the discovery of a number of early solid-state laser systems, in the original formulation of the theory of nonlinear quantum optics; in proposing and explaining mode-locked ultrashort-pulse lasers, GaAs optoelectronics; in proposing and demonstrating semiconductor-based integrated optics technology; in pioneering the field of phase conjugate optics; and in proposing and demonstrating the semiconductor distributed feedback laser. He has published widely in the laser and optics fields and has written a number of basic texts in quantum electronics, optics, and quantum mechanics.

Dr. Yariv is a member of the American Academy of Arts and Sciences, the National Academy of Engineering, and the National Academy of Sciences.